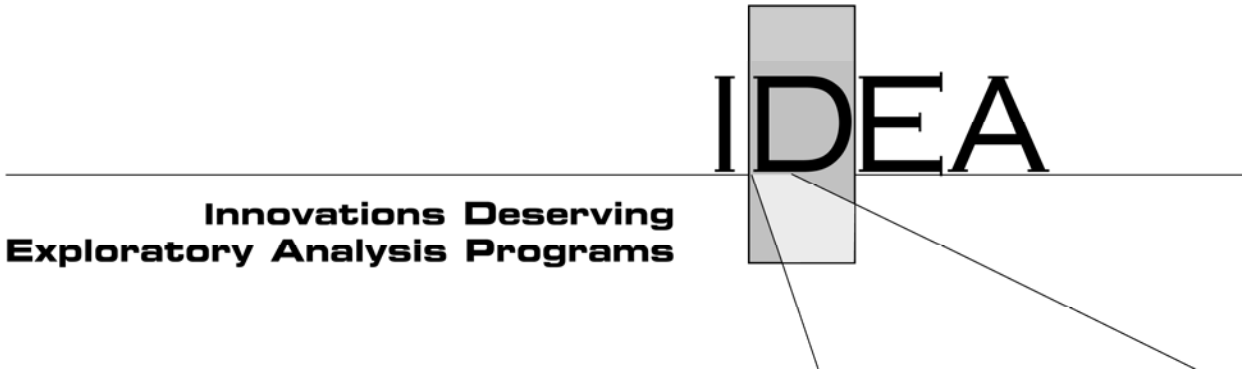

High-Speed Rail IDEA Program

Handheld Wheel Flaw Detection Device

Final Report for High-Speed Rail IDEA Project 39

Prepared by:
Zack Mian
International Electronic Machines

July 2004

TRANSPORTATION RESEARCH BOARD
OF THE NATIONAL ACADEMIES

INNOVATIONS DESERVING EXPLORATORY ANALYSIS (IDEA) PROGRAMS MANAGED BY THE TRANSPORTATION RESEARCH BOARD

This investigation was performed as part of the High-Speed Rail IDEA program supports innovative methods and technology in support of the Federal Railroad Administration's (FRA) next-generation high-speed rail technology development program.

The High-Speed Rail IDEA program is one of four IDEA programs managed by TRB. The other IDEA programs are listed below.

- NCHRP Highway IDEA focuses on advances in the design, construction, safety, and maintenance of highway systems, is part of the National Cooperative Highway Research Program.
- Transit IDEA focuses on development and testing of innovative concepts and methods for improving transit practice. The Transit IDEA Program is part of the Transit Cooperative Research Program, a cooperative effort of the Federal Transit Administration (FTA), the Transportation Research Board (TRB) and the Transit Development Corporation, a nonprofit educational and research organization of the American Public Transportation Association. The program is funded by the FTA and is managed by TRB.
- Safety IDEA focuses on innovative approaches to improving motor carrier, railroad, and highway safety. The program is supported by the Federal Motor Carrier Safety Administration and the FRA.

Management of the four IDEA programs is integrated to promote the development and testing of nontraditional and innovative concepts, methods, and technologies for surface transportation.

For information on the IDEA programs, contact the IDEA programs office by telephone (202-334-3310); by fax (202-334-3471); or on the Internet at http://www.trb.org/idea

IDEA Programs
Transportation Research Board
500 Fifth Street, NW
Washington, DC 20001

Handheld Wheel Flaw Detection Device

IDEA Program Final Report
for the Period August 2002 through March 2004

Contract Number HSR-39

Prepared for
the IDEA Program
Transportation Research Board
National Research Council

Zack Mian
International Electronic Machines

July 7, 2004

Table of Contents

Acknowledgements

Many people contributed to the work described in this report. IEM would like to thank them all, including:

Chuck Taylor for the TRB
Greg Garcia, Bob Floram, and ***Paul McMahan*** for the TTC
Pat Ameem and ***Larry Benedict*** for the AAR
Ken Staltz and ***Bob Blank*** for the Norfolk Southern
Jerry Manager for Union Pacific
Dr. Greg Martin for CSX
Glen Brandimart for Olympic Railway Services
John Popovich for Griffin
And all of IEM, including ***Zack Mian***, ***Bill Peabody***, ***Robert MacAllister***, and ***Ryk E. Spoor***

Abstract

The inability to accurately and reliably determine the condition of a railway wheel leads to a number of negative consequences, ranging from time and effort wasted servicing wheels that do not need it (either because they were actually good, or because they are too flawed to return to service) to accidents caused by flawed wheels. Current ultrasonic inspection technologies have a number of key flaws mostly due to their need for a liquid or gel couplant and for fixed-location power sources. International Electronic Machines Corp. (IEM), having produced a promising conceptual demonstration, developed a prototype for an EMAT (electromagnetic acoustic transduction) based Portable Wheel Flaw Detection Gauge.

The resulting prototype demonstrated the ability to reliably, repeatably, and accurately determine the condition of a railway wheel's tread or flange with a portable, rugged device, with the potential to do the same to other wheel components. During this project IEM created designs for signal pulsers, preamplifiers, power supplies, sensor heads, and many other necessary components, as well as incorporating multiple signal analysis algorithms, an expert system to identify types of flaws, and a graphic user interface.

Keywords

EMAT, noncontact, flaw detection, railroad wheels, digital signal processing

Executive Summary

International Electronic Machines Corp. (IEM) developed a portable Wheel Flaw Detection Gauge based on EMAT (ElectroMagnetic Acoustic Transduction) technology. The prototype developed in this project provided reliable and accurate detection of flaws on and through wheel tread. IEM demonstrated that with a different sensor head – which could be designed for simple exchange – flaws on the flange could be located equally quickly and reliably; preliminary experiments also demonstrated that the same technology and approach would be able to find flaws in all other parts of the wheel, such as the rim and plate. This technology is of importance to:

- Improve the safety of railroads by detecting flaws in wheels before the flaws can cause breakage; broken wheels account for many millions of dollars in accident costs every year (see FRA data at safetydata.fra.dot.gov), and undetected flaws in wheels are a significant cause of wheel breakage. Breakages can lead to derailments, and such derailments are of increasing concern due to increasing axle loads, especially on lines used by high-speed passenger trains.
- Reduce operating costs by ensuring that only wheels that have repairable flaws or conditions are serviced, while those with condemnable flaws are eliminated from service, and that no good wheels are subjected to unnecessary turning and servicing.

In preliminary work on this project, IEM demonstrated that such equipment could be made portable and that it was possible to detect tread flaws in railroad wheels utilizing this technology. Current technology uses piezoelectric acoustic transducers, which require a liquid or gel couplant to transmit the signal to the wheel, giving rise to many difficulties with this technology – refraction of the signal at the boundary, variable couplant performance dependent on temperature, and sensitivity to dirt and surface conditions. EMAT technology eliminates these problems as the electric and magnetic fields interact in such a way as to permit an electric field to generate pulses of ultrasonic waves directly into a metallic object (such as a railway wheel) without requiring any physical contact or medium to transfer the pulses back and forth. Thus an EMAT-based device can send and receive signals at any temperature, in any weather, and even through surface coatings, grease, paint, and surface flaws such as spalling and shelling.

While a pre-prototype demonstrated the basic feasibility of the concept, it required a complete reworking to become a functional, practical prototype. This involved the design and development of unique sensor heads, EMAT pulsers, controllers, digital signal processor-based boards, coil designs, power supplies, signal filters, and other ancillary hardware, as well as the creation of robust, innovative, and proprietary software for noise filtering, signal reception and enhancement, feature detection and analysis, including expert system design, fuzzy logic coding, and the design of an effective user interface. In addition, IEM designed the Wheel Flaw Detection Gauge to withstand the rigors of field use, as instruments for use in train yards will inevitably be subjected to considerable impact, stress, and wildly varying temperature, humidity, and precipitation conditions.

IEM produced a prototype of the Wheel Flaw Detection Gauge and tested it in laboratory and field settings on different wheel sets with conditions ranging from brand new to condemnable flaws. The Wheel Flaw Detection Gauge demonstrated accurate, reliable performance, recognizing and localizing multiple types of flaws, not being fooled by minor surface conditions, passing all good wheels, and producing the same results on each wheel in multiple readings, thereby demonstrating that its readings are consistent, reliable, and accurate.

Further development is needed to finalize the commercial design of the Wheel Flaw Detection Gauge. This includes the design of sensor heads for rim and plate inspection, the creation of a mechanism to allow the easy exchange of these sensor heads in the field, a finalized casing and component design that will minimize size and weight, custom lithium-based battery packs for longer battery life in a smaller unit, ergonomic/usability testing, and extensive field testing of the unit with railway personnel to provide feedback for refinements in convenience and responsiveness.

The Need For A Portable Wheel Flaw Detection Device

Importance of Inspections

In the railroad industry, wheel defects and failures caused by time and wear are a significant cause of derailments. Detection of defects and wear-related flaws before such accidents occur, therefore, is an important issue. In addition, it is important to be able to accurately detect and identify wheel flaws of various kinds to prevent unnecessary time, money, effort, and wear on expensive truing equipment on a wheel that should be simply removed from service.

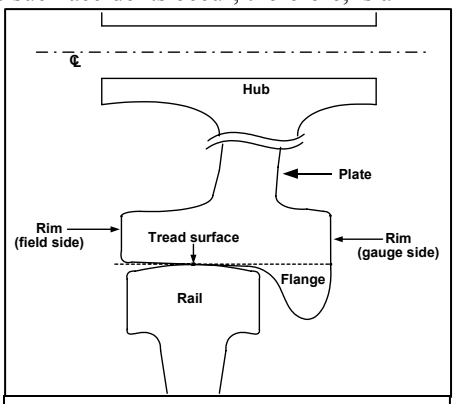

Figure 1: Railway wheel features

Quick Primer on Wheels and Flaws

Figure 1 shows a compressed cross-section through a typical railway wheel on a rail. Starting at the center and working outward, the wheel consists of a hub, a "plate" section (analogous to the spokes of a bicycle wheel, but a solid piece of metal), the rim (which has a "field", or outward edge, and a "gauge", or inner edge), the tread (which is the part that contacts the rail itself), and the flange, which is the overhanging part of the wheel that keeps the wheel securely on the rail.

While these wheels are made of extremely hard steel, they are also subjected to tremendous stresses and can develop a number of flaws, including thermal cracks (fractures caused by localized heating), gouges, spalling and shelling, and other wear-related flaws and features such as hollow tread. A few of these are shown in **Figure 2**.

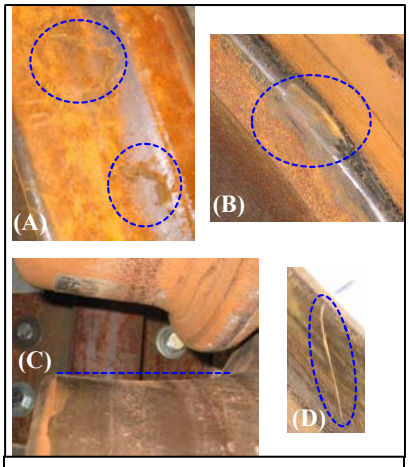

Figure 2: Wheel flaws/wear: (A) shelling, (B) gouge, (C) hollow tread, (D) machined cut simulating crack

The current practice of inspecting wheels is based on the AAR guidelines as they appear in the Manual of Standards and Recommended Practices, G-18. These guidelines recommend the use of two piezoelectric ultrasonic sensors with an appropriate couplant to interrogate the tread surface from the side of the wheel as well as from the running surface of the wheel. However, the present practices do not evaluate cracks in the wheel flange, wheel plate, or cracks in the wheel tread along the cross-section of the wheel. Unfortunately, these three defect types account for many wheel-related failures.

Moreover, there are several current trends that have been and are continuing to increase the overall stress and wear on wheels, and that thus will lead to increasing numbers of fatigue-related failures:

1. **Increasing car loads.** A continually growing proportion of the rail fleet consists of 125-ton and greater cars; it is possible that this trend will increase.
2. **The growth of double-stack service with as-yet unknown stresses on wheels.** While it is still too early to evaluate the effect of this traffic, the simple physical geometry shows that this method of rail shipping changes the force distribution on the wheels in significant ways.
3. **Increasing use of flange lubrication.** This reduces wear on wheels as well as on the rails, thus reducing the perceived need for replacement of the wheels and increasing the overall chances that older wheels will suffer a fatigue-related failure.
4. **The use of harder steels in rails.** While the harder steels reduce wear on the rails, they potentially increase the effective wear on the wheels that run on these rails.

Clearly, therefore, it is of great importance that a device and method be developed to detect the various forms of wheel flaws that can lead to failure. To ensure both acceptance and use within the industry, any device to perform this task must be accurate, reliable, inexpensive and, most importantly, both fast and easy to use. Unfortunately, no such device currently exists. Extant devices fulfill virtually none of these requirements, and are also limited in the areas of wheel to which they can apply. From IEM's communications with the TTCI, important areas for the detection of flaws in freight wheels are the tread, flange, and rim. No current-art systems can interrogate any portion of the wheel other than the tread. One such system, for example, will indicate certain flange conditions, such as "high flange", but will do so based solely on tread condition (i.e., a flat spot on the tread indicates a strong likelihood that the flange is high at that point), and must make assumptions (such as a perfectly circular flange) in order to do so. In addition, as described below, current-art ability to detect flaws even in the tread is significantly limited.

Wheel Accidents are Expensive

As mentioned previously, wheel accidents are considerably more expensive per incident than the average equipment failure incident. All told, in the five year period from 1998 through 2003, ***wheel failures*** accounted for a loss of over **$73,000,000**, many such failures due to ***undetected flaws*** in flange, tread, and rim (based on the FRA's data at http://safetydata.fra.dot.gov/OfficeofSafety). If ***any*** significant fraction of these accidents could be prevented by proper inspection, the savings to the industry would be substantial. This savings would very likely rise over time, since – as detailed previously – there are a number of industry trends that are virtually certain to cause an increase in the number of fatigue-related wheel failures. These savings figures do not include the considerable amount to be accrued through ensuring that maintenance is done only on known-good wheels rather than on wheels that are discovered to be flawed only after some work has been expended on them.

Problems Associated With Current Practice

While current wheel inspection techniques and statistics are considerably superior to those of several decades ago, there are still a number of avoidable failures of wheels every year. Several factors in the current technology contribute to this problem.

User-Unfriendly Systems

Current inspection systems, mostly based on conventional ultrasonic technology, are not designed to be user-friendly and require considerable interpretation. Often, the current systems (such as the one shown in **Figure 3**) are physically difficult to use, requiring the wheel to be removed and rotated through an entire turn, or more, in order to obtain full readings. User-unfriendliness has three negative consequences:

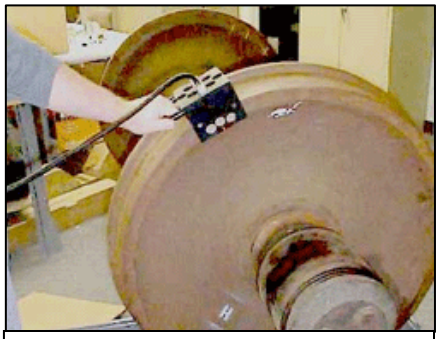

Figure 3: Ultrasonic Wheel Inspection Probe

1. **Cost.** The end-users must be extensively trained; this costs time and money.
2. **Increase in Errors.** Any complicated measurement that requires training and judgment carries with it a greater chance of a confused or misunderstood reading.
3. **Reluctance in Acceptance.** Introducing new technology to any field is likely to meet with resistance from the work force, especially if the technology is inherently difficult to use.

Line-Powered Sensors

In a field setting, the most convenient instruments to use will be those that are smallest and most portable, while retaining all of the functionality of other, less portable instruments. Current ultrasonic inspection systems, such as the system shown in **Figure 3**, are tied to large power supplies, generally standard 110V-AC or a semi-portable system that supplies this same voltage. This renders them cumbersome, if not completely unsuitable, for portable "walk-around" inspection applications.

Waveform Restriction

Different sections of a wheel, and different types of flaws, can require multiple types of waves or configurations of sensors to detect them. Unfortunately, most current-art devices are limited in the waveforms they will produce, and cannot produce a number of wave types that would be useful in this application.

Essential Technology Limitations

Perhaps the greatest current-art problem stems from ultrasonic technology itself. Standard ultrasonic inspection techniques, while certainly far superior to prior methods, carry with them certain inevitable drawbacks that are intrinsic to the technology.

Application of Couplant

The first and most obvious difficulty is the application of the couplant to the wheel. Even under otherwise ideal conditions, the couplant itself places extra demands on the user, as:

- A supply of couplant must be carried and maintained.
- The couplant must be kept beneath the transducer in sufficient quantity.
- The couplant is generally sensitive to temperature changes. As train yards (and thus their wheels) can vary in temperature from -40ºF to +120ºF, this can present a major practical problem.
- Even automated, the application of couplant tends to slow the process of taking readings by a considerable factor.

Sensitivity to Contamination

The above difficulties all assume that the couplant itself is usable. However, in real life railroad wheels are often covered in dirt, grime, and oil, with other materials randomly appearing in the mix. Applying the couplant to such wheels carries with it a high risk of contamination. The problem with this is that the control and use of the ultrasonic signals is highly dependent on the acoustic characteristics of the couplant, and these characteristics can be drastically altered – in unknown fashions – by the presence of contaminants.

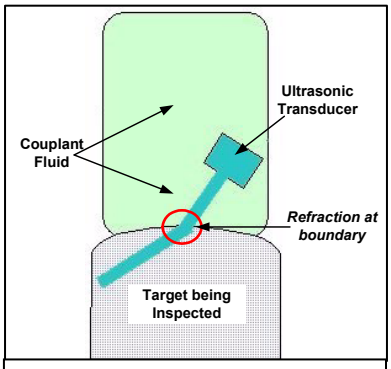

Figure 4: Refraction of sound beam at couplant/target interface

Signal Transmission Limitations

Even leaving these problems aside, traditional methods of ultrasonic inspection have one other major weakness. Couplant is present in order to deliver the ultrasonic signal to the wheel in sufficient strength to be clearly readable; however, this requires that the signal traverse the boundary between two different media: the couplant and the target. This requirement causes refraction at the boundary between the two media, in precisely the same manner and for precisely the same reasons as refraction occurs with light traversing the boundary between air and water or glass. As seen in **Figure 4**, the piezoelectric transducer generates an ultrasonic beam that is noticeably refracted upon entering the target. The net effect is that it becomes extremely difficult for a traditional ultrasonic device to interrogate the target beneath the shallow surface layer.

Solution: Portable EMAT-based Wheel Flaw Detection

International Electronic Machines (IEM) Corp proposed the design and construction of an electronic method of non-invasive wheel inspection based on Electro-Magnetic Acoustic Transduction (EMAT) technology. This proposed system would be low-cost, battery-powered, simple to use, reliable, and rugged enough for use in the field; it would eliminate the shortcomings of the current art devices described above, while offering both performance and price advantages.

IEM's Approach

To properly describe IEM's approach, it is necessary to understand EMAT technology.

Basic Principles of EMAT Operation

The functioning of an EMAT device is based on the fact that changing electric fields generate magnetic fields, and vice versa, in conductive media, that such fields can exert force on the medium – and that, therefore, movement of the medium can and will induce electromagnetic fields/currents in a conductor under the right circumstances. The combination of these principles makes possible a transducer – a device that can convert electromagnetic impulses to vibrations in the target medium, and that can then take vibrations of that medium and convert them into electromagnetic impulses again. A more accurate and detailed description is given below, based on the introduction to EMAT technology given in **PB81-109514**, *Development of a Prototype EMAT System for Inspection of Rails* (Rockwell International, 1980).

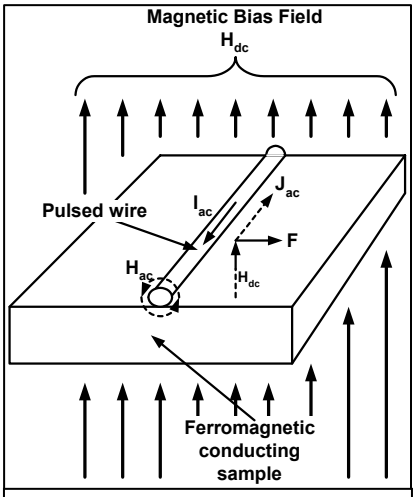

Figure 5: Basic EMAT principle

Figure 5 shows a pulsed wire that induces a magnetic field $\mathbf{H_{ac}}$ that, in turn, induces an eddy current $\mathbf{J_{ac}}$ in the near surface of nearby conducting sample. If a separate bias magnetic field $\mathbf{H_{dc}}$ is imposed over the same region with the right geometry, the combination of the bias magnetic field and the eddy current produces a sideways force on the eddy current. This force is then transferred to the lattice of the sample with the same frequency as the original pulsed current in the wire.

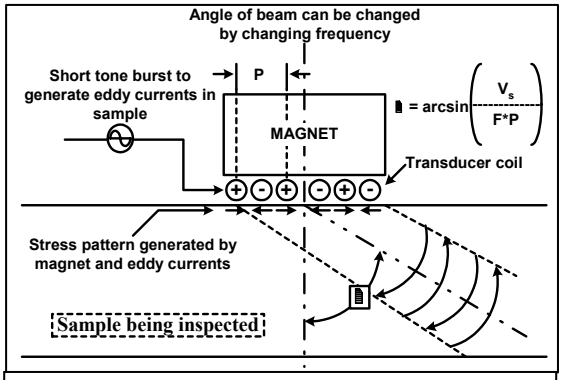

Figure 6: Propagation of ultrasonic beam from EMAT

If the geometry of the transducer coil and its current are repeated with alternating signs under the bias magnet, the pattern of instantaneous lattice forces that are produced within the test object propagates as an ultrasonic beam. This is illustrated more clearly in **Figure 6**. The directions of the propagation and polarization of this beam are determined by the geometry of the EMAT coil, or more specifically, the pattern of the eddy currents that are induced in the surface of the test object by the coil, and the direction of the bias magnetic field vector at the surface of the part. This mechanism of generating the ultrasonic beam within a surface layer of the test object itself, rather than in the transducer, is why an EMAT does not have to be in physical contact with a conductor to generate or receive an ultrasonic beam. However, the EMAT coil must be close to the part since the magnitude of the eddy currents, hence, that of the ultrasonic beam, decreases approximately exponentially with the separation distance (lift-off).

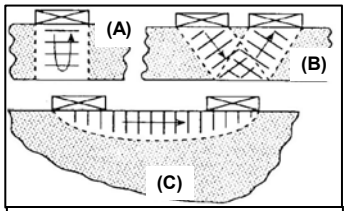

Figure 7: Pulser/Receiver transducer configurations

The periodicity of the EMAT coil, P, the frequency of the electrical tone burst, F, and the shear wave velocity in the sample, V_s, control the propagation direction of the shear wave produced by an EMAT. The propagation angle of the shear wave is determined by the relation shown at the upper right in **Figure 6**: 2 = arc sin (V_s/FP). This figure illustrates the mechanism of ultrasonic beam forming by an EMAT transducer.

Radio frequency pulses in the EMAT coil generate eddy currents in the wheel surface. The interaction of the eddy currents and the static magnetic field generates ultrasonic energy that is beamed

within the wheel, and produces echo signals from cracks and other irregularities in the wheel. The returning echoes interact with the magnetic field at the wheel surface, creating an echo pulse in the EMAT coil that can be used to determine the presence and magnitude of defects encountered by the beam. These signals can be sent and received in different configurations, as shown in **Figure 7**. **Figure 7A** depicts a transducer being used for both send and receive – a method called the "pulse-echo" or monostatic approach, while **7B** and 7**C** both have different transducers in the send and receive roles – the so-called "pitch-catch" or bistatic approach. The latter approach lends itself well to differing angles of interrogation, as shown.

This, combined with the ability to control the propagation angle via frequency as depicted in **Figure 6**, graphically illustrates how beam scanning can be performed electronically, merely by changing the driving frequency rather than mechanically tilting the scanning head, which can be useful and more convenient for some applications, such as changing the interrogation angle and depth into a wheel.

Advantages of EMAT Approach

EMAT has three significant advantages over ultrasonic testing equipment using piezoelectric transducers. These are that it requires no liquid couplant, it can see "through" spalling/shelling and surface fractures, and it is not distorted by standard acoustic signal refraction problems.

No Liquid Couplant

Since they do not require a couplant to transmit the ultrasonic signals, EMAT based systems:

1. Have the potential for operating at greater speeds in areas where the wheel has been treated with lubrication grease, as there is no requirement to clean the wheel in order to ensure a proper coupling as may be necessary when using classic ultrasonic sensors.

2. According to Oscar Orringer (*Rail Testing: Strategies for Safe and Economical Rail Quality Assurance*, Transportation Research Record, 1174, pp 28-42) "EMAT transducers subject the rail to a DC magnetic field together with a pulsed RF Signal. These two electromagnetic components combine to generate ultrasound and receive return signals directly in the railhead; thus the refraction problem is avoided. Electromagnetic transduction between the rail and the probe also suggest that EMAT systems will tolerate heavy lubrication interference better than conventional systems." For purposes of wheel flaw detection, this is significant, as it shows that the absence of the couplant eliminates the refraction effect that is deleterious to conventional ultrasound interrogation of wheels.

3. Maxfield, Kuramoto, & Hulbert (*Evaluating EMAT Designs for Selected Applications* Mater. Eval., 45, 1166-1183 (1987)) add, "It is sometimes possible to work with liftoff distances (separation between sensor and rail) of 3 mm (0.125") or more." While this is more useful for moving applications, a large potential liftoff distance permits the EMAT to operate through significant layers of burned-on grease, paint, and other contaminants.

See Beneath Head Checks, Shelling, and Surface Fractures

Work performed by North American Rockwell has shown that its 90 degree shear wave system EMAT is able to "skim along just under the surface and reflect strongly from transverse flaws that lay close to the surface even though the rail surface may be covered with small cracks or checks that reflect the Shear Vertical (SV) waves used by conventional transducers". Again, this demonstrates one of the major advantages of EMAT technology, in that it shows that surface flaws that can severely interfere with conventional ultrasonic interrogation of metallic structures are no impediment to an EMAT-based approach. IEM has verified that this applies to the common wheel condition of shelling.

Not Distorted by Acoustic Coupling Refraction

Some of the waveform modes such as a true SH0 mode are only achievable through using an EMAT sensor. The angle of attack of standard piezoelectrically induced ultrasonic beams can be distorted by minor changes in the position of the sensor relative to the rail. EMATs are less susceptible to this distortion.

Challenges Presented by EMAT Approach

Prior IEM work summarizes the significant disadvantages of EMAT systems as follows:

Lift-off Sensitivity

With any acoustic or electromagnetic signal, the strength of the signal varies roughly with the square of the distance between the source and the receiver. With EMAT, however, there is a complication introduced due to the fact that the actual signal interrogating the wheel is being generated by the interaction of another signal with the wheel, and that the signal being processed in the main system is generated by the interaction of the interrogated wheel with the receiving EMAT field. In effect, there is more than one inverse-square factor involved – the emission from the EMAT pulser to the wheel surface, then the transit of the resulting ultrasonic waves through the wheel, and then the emission of electromagnetic waves from the wheel to the receiving EMAT transducer. This means that any increase in distance from the wheel surface can have a drastic effect on the strength of the signal sent into the wheel and returning therefrom. Still, as mentioned earlier, lift-off is a relatively minor concern in this application and more than sufficient lift-off has been demonstrated for purposes of this application.

Inefficiency

EMATs are relatively inefficient at generating ultrasonic energy when compared with piezoelectric transducers, which are used in standard ultrasonic inspection. This, in turn, results in relatively poor signal-to-noise ratios (S/N). The S/N ratio, however, can be improved upon using a number of signal processing techniques.

Detecting Wheel Flaws with EMAT

The detection of a wheel flaw through EMAT functions very similarly to that of any acoustic-based detection technique. **Figure 8** shows a simplified version of the way in which such detections are accomplished.

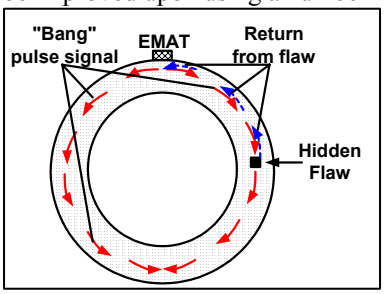

Figure 8: Detection of a flaw inside a wheel

A pulse is sent out from the EMAT unit. This pulse proceeds to travel around the circumference of the wheel in both directions. As the speed of sound in various materials, including steel, is well-known, the time from the initial "bang" to the sound of the returning original signal can be precisely calculated. If a flaw exists in the wheel at any point between the traveling signal and its return to the sensing location, a portion of the energy of the pulse will be reflected back. This "return" signal will inevitably reach the EMAT sensor before the original signal finishes its traverse of the circumference of the wheel. Thus, to detect the flaw involves "listening" for signals that occur between the initial "bang" and the successive returns of that original signal to the EMAT location. The only exception is if a flaw exists at the point precisely opposite the EMAT, where both waves cross paths; a return from such a flaw will, of necessity, arrive at the same time as the original signals and will therefore be lost in the noise of the returning main signal. Therefore, to eliminate this possibility, it is almost always necessary to take two separate readings, at slightly different locations on the wheel, so as to be able to detect flaws in this small "dead zone".

In actuality, of course, the process is more elaborate, as the signals can be reflected from the internal surfaces, spread out and decay over time, and so on, necessitating multiple samples, signal filtering and enhancement, and other techniques to obtain clear and unambiguous results, but the basic principle remains as illustrated above. **Detailed discussion** of the various signal processing techniques used in the Portable Wheel Flaw Detection Gauge will be found in the discussion of "***Algorithm/ Software Design and Testing***" under the Results section.

IEM's Criteria for an EMAT-Based Portable Wheel Flaw Detection Gauge

IEM's Portable Wheel Flaw Detection Gauge must offer more performance than any current-art device while overcoming their shortcomings. Therefore, it should:

- **Be entirely portable.** IEM's device should be something a user can carry around and use

without need for any outside support.

- **Require no couplant.** This is in fact an inherent advantage to the selected EMAT approach.
- **Interrogate the entire wheel with one or two swift applications.**
- **Be unaffected by the presence of dirt or contaminants.**
- **Be unaffected by surface conditions such as rust, paint, burned-on grease, and so on.**
- **Provide a user-friendly interface.**
- **Be highly reliable.**

IEM demonstrated, prior to the commencement of this project, that such a device was theoretically possible. Our pre-prototype unit was able to send an interrogation pulse around the entire circumference of a railroad wheel and determine the location of a pre-known fault along that circumference, with a single application of the pre-prototype on one point of the wheel. As detailed in our Patent #6523411, IEM also has designed and tested a static, in-ground version of this technology. The pre-prototype's components were, unfortunately, quite incapable of providing the performance needed in signal generation, detection, analysis, and so on; it sufficed only to demonstrate that a Portable Wheel Flaw Detection gauge was POSSIBLE. In order to accomplish these goals, this proposed gauge should include the following elements:

1. **Multiple EMATs each having a transmit coil** to propagate an ultrasonic wave into a wheel and a receiving coil to receive an ultrasonic surface wave from the wheel.
2. **A *portable battery operated EMAT pulser* (presently not commercially available)** for exciting the EMAT and producing an ultrasonic wave in the wheel.
3. **A computer control unit connected to and communicating with** the pulser (radio frequency generator) and the EMAT.
4. **A data acquisition unit** connected to and in communication with the computer control unit and the EMAT assembly for determining defects in the wheel.
5. **A digital signal processing (DSP) system** to interpret the ultrasonic waveform data so that flaw data can be shown in easy to understand reports. The DSP will also provide superior data analysis not available by present techniques.

Results of Work

Overview

The development of a new instrumentation product such as the Wheel Flaw Detection Gauge is a complex process. The process use in this project was as follows:

- **Specifications development** – the creation of a clear description of all major aspects of the proposed device's performance and physical requirements; this also includes meetings with interested parties
- **Hardware selection/design, assembly, and testing** – the selection of appropriate components to create a device capable of meeting the specifications, or, if required components do not exist, the design and manufacture of these unique components, and subsequent testing on the hardware to determine that it can and does perform as expected
- **Software design and testing** – the creation of applications/programs that will perform all of the functions detailed in the specifications, and testing these applications to ensure they perform as required
- **Prototyping, refinement, and field testing** – the creation of a fully-functional version of the device, testing and elimination of any last-minute difficulties, and analysis of the test data to determine how well the prototype met the specifications.

Expert Review Panel

A panel of experts from railroads, TTCI, AAR, and wheel manufacturers was established to provide guidance for the project. Panel input included useful information from TTCI on the areas of interest for the AAR wayside crack detection system, which helped verify IEM's technical direction in this project. As tread and flange flaws were of interest and IEM's wayside work had already begun to target those areas, it was decided that the Portable Wheel Flaw Detection Gauge would also begin with a focus on

those areas, and expand to cover the rest of the wheel after the basic design and development had been completed. It appeared likely that the majority of the work to be done on the other wheel areas would be the design of other sensor heads, rather than any other major theoretical work.

Specifications

Starting from our prior work in the EMAT NDE field, our pre-prototype results, and our knowledge of the railroad industry, IEM developed a set of preliminary specifications. Following this, IEM then met with or contacted a number of interested parties to refine and update these specifications. The result of this effort was a comprehensive practical specification for the Wheel Flaw Detection Gauge, reflecting both the performance and physical requirements to make the device useful and acceptable in the industry. These specifications, along with how well IEM's final prototype met them, are shown in full in **Conclusions** (Table 2).

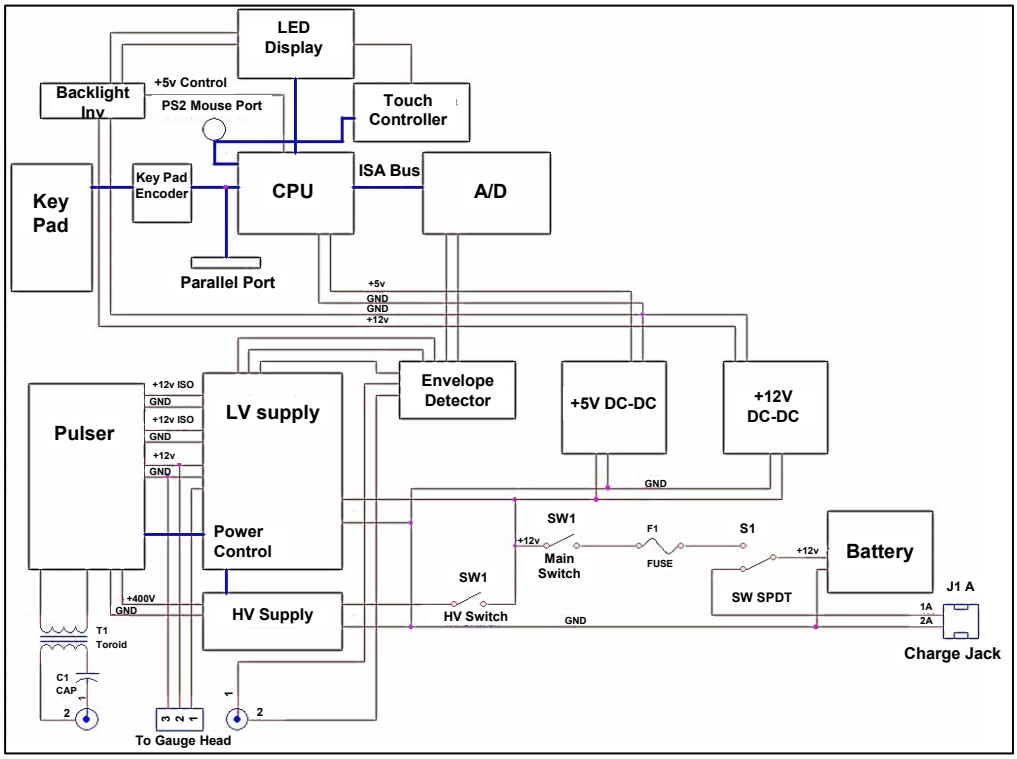

Figure 9: Block Diagram of Portable Wheel Flaw Detection Gauge design

Hardware Design and Testing

Figure 9 is a block diagram of the design of the Portable Wheel Flaw Detection Gauge. The hardware design for the portable Wheel Flaw Detection Gauge consists of a total of five major components:

1. **Sensor or gauge head.** This is the actual working "contact" section of the gauge, in which the EMAT units are situated and perform the send/receive function on the wheel.
2. **Pulser unit.** The pulser generates the signal that is used by the transmitting EMAT; thus it is the pulser that determines the power and frequency of the "bang" sent into the wheel for detection purposes.
3. **Preamplifier unit.** The preamplifier takes in the received EMAT signals and prepares them for amplification; by specific processing approaches the preamplifier can very significantly reduce noise.

4. **Power Supply.** Various components within the system will require different voltages and currents; a properly designed power supply distributes the power from the batteries efficiently.
5. **Controller unit.** The controller is the user interface and associated electronics that permit the user and the gauge to effectively interact, with the gauge providing readings and the user adjusting the parameters and storing/retrieving data as needed.

Sensor Head

The sensor head is the "eye" of the system; it actually induces the signals into the wheel and receives the return signal. It is also the most likely component to be damaged, as it must be applied to the wheels and removed from them, resulting in a high probability of being dropped on rails, banged against wheels or other train components, and so on. The nature of the EMAT process, moreover, requires powerful magnets that require considerable force to remove from wheels. The sensor head, therefore, consists of two mutually dependent subsystems: the EMAT components, which perform the actual sensor work, and the mechanical support components, which both protect the electronics and are designed to facilitate the use of the sensor head; due to the facilitation role, these are discussed in the later "**Usability Issues**" subsection. **Figure 10** shows an exploded view of the sensor head and all components.

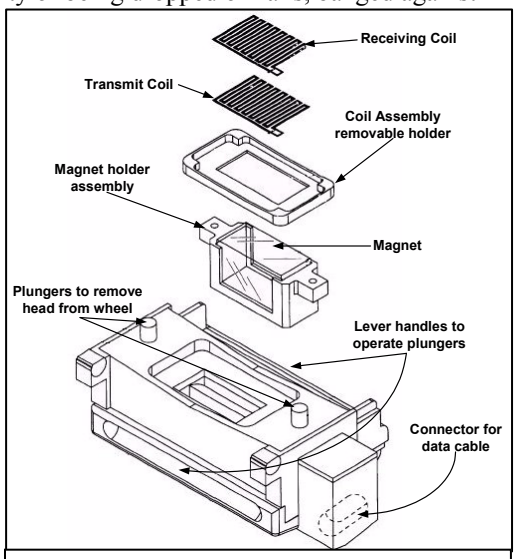

Figure 10: Sensor head showing all components

EMAT Components

There are **three components** of the actual EMAT system present in the sensor head. The first is the ***magnet***, which is required as described earlier to permit the induced eddy currents in the sample to generate acoustic signals. This is an extremely powerful permanent rare-earth magnet that provides an excellent bias field for EMAT operation. Despite its small size – roughly1x1x2 inches – the magnet is powerful enough to make it extremely difficult to remove the sensor head from the wheel. This necessitates particular design features, detailed in **Usability Considerations**, to facilitate the removal of the sensor head from the wheel once readings have been obtained.

The other two components are the ***coils*** – one to transmit the signals, the other to receive the return pulses. As described in the "Basic Principles of EMAT" section, the same coil designs can be used to receive the return signals as to transmit the initial signals. These coils, shown in **Figure 11**, are IEM custom-designed EMAT transducer coils encased in a protective plastic casing. Without the plastic casing, the coils would be easily damaged during the process of taking readings. While the basic coil circuits are a sandwich, with Kapton® plastic on either side, they are not particularly resistant to wear. IEM added a layer of PEEK (poly-ether-ether-ketone) plastic. IEM has tested this design in hundreds of wheel readings, and while wear does occur, the wear process is extremely slow and IEM estimates that many thousands of wheels could be read with any given set of coils before there would be any probability of wear-through, as long as very basic precautions were taken with the readings (see **Usability Considerations**).

Figure 11: Custom IEM EMAT coil

Pulser

As noted in our Background section, IEM has had experience in creating EMAT systems previously. The demands of this particular application, however, were unique and imposed rigorous restrictions on the design of the EMAT unit, especially with respect to the pulser design, as there was not, at the time, any portable pulser unit that would meet the power or size requirements.

Pulser Operation and Requirements

The heart of the system, the pulser, as its name implies, generates pulses of electrical signals that are sent through the coil to create the EMAT signal. A pulser must generate signals at high frequency in order to create high-frequency sound waves in the target object. The frequency, as mentioned earlier, determines the interrogation angle of the sound beam and determines the minimum size of flaw/feature that can be detected by the system. Given the speed of sound in steel, this demands a high-frequency pulse of 500,000 Hz or even more to resolve flaws that are on a centimeter scale.

The physics of EMAT operation also place another demand on the signal generation source. All electromagnetic phenomena obey the inverse-square law of intensity; in the case of EMAT, this works against the technology because the induction of the signal must be done across some distance X from the actual surface, and then the return signal must be sensed across the same distance X from the surface. To counter the inefficiency, it is therefore desirable to generate the pulses at very high power, increasing the return signal and making the signal easier to sense and analyze.

Finally, even with relatively high-power pulses, the return signals tend to be very low power and thus can be adversely affected by noise present during reception. This is one of those technical problems that often presents an apparent paradox; one needs high-frequency, high-power pulse generation, but that generates noise that can overwhelm the signal in the sensitive receivers… and so one tries to increase the power to get more signal, which creates more noise in the detection electronics, and so on. These challenges had to be confronted in the development of IEM's portable EMAT technology.

IEM's Original Pulser Design

At the time of initiating this project, IEM had a pulser design that had demonstrated some promise in a related project for the New York State Energy Research and Development Authority (NYSERDA). However, for purposes of the Portable Wheel Flaw Detection system, it became clear that it had a number of flaws that made it unacceptable for this application:

1. **Insufficient power.** The previous pulser unit could develop power of approximately 800 watts. IEM's calculations showed the portable unit would require at least 2500 watts to guarantee a clear signal.
2. **Excessive size.** The previous pulser unit, while considerably smaller than other commercial units (see the RITEC pulser discussed below), nonetheless was nearly as large as IEM considered acceptable for the entire controller unit, which was to incorporate the pulser, preamplifier, power supply, and user interface.
3. **Fixed mount power supply.** The then-current pulser unit was dependent on standard A/C power to run it.

In addition, as the prior unit was intended for use at a fixed location with fixed power supplies, its electronics were not designed to be as robust and tolerant of electrical variations, shorts, and so on as should be the case for a portable unit meant for long-term hard use.

RITEC Pulser

While working on EMAT designs for the Rail Flaw Cart (mentioned previously), IEM researched a number of sources for new pulser technology. The culmination of this search was the choice to work with RITEC (a company with considerable experience in this area) and obtained RITEC's OEM package, allowing us to assemble the components in a configuration that was most appropriate for our purposes. The RITEC pulser unit resulting from this possessed several positive traits when compared to the prior unit – a peak power of 5KW and a wide range of operational frequencies up to 20MHz. Despite these advantages, the RITEC pulser unit had one major practical disadvantage: **size**. Assembled, with all ancillary equipment, the RITEC unit was large enough to take up an entire drop-in payload bay, such as those for mobile units like IEM's Rail Flaw Inspection Cart. In addition, the RITEC pulser required a standard AC power source. Accordingly, IEM began to explore the possibility of designing our own miniaturized custom pulser for the EMAT units.

IEM's Custom Mini-Pulser

IEM believed it was possible to design a pulser unit that was far smaller and would still develop the same level of power with no more distortion. Further research into the design of pulsers led us to believe that a design based around MOSFET technology would prove effective.

Results of Mini-Pulser Design

IEM's custom mini-pulser, whose main PCB is shown in **Figure 12**, is a twin-channel design capable of developing over 2500 watts per channel, with an integral bridging capability that permits a combined pulse of over 5kw, equal to that of the RITEC pulser. It is frequency agile and usable with many different EMAT designs. Despite this tremendous performance, the pulser and requisite power supply connections now fits into a space barely the size of two fists, considerably smaller even than IEM's prior custom design, and uses considerably less energy. In addition, the electronics of this pulser are extremely robust against incident electrical signals.

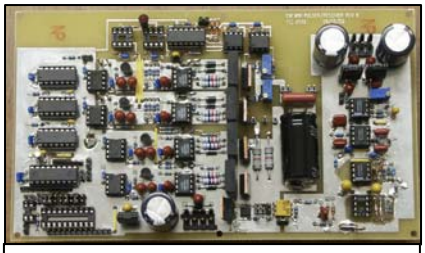

Figure 12: IEM's Mini-Pulser main circuit board

Preamplifier

Preamp Design

One source of noise can come from the actual transmitting electronics; the other major source comes from the received signal – both the signal itself and the electronics used to capture it. IEM designed its own custom preamplifier and receiver to minimize noise. Earlier COTS-based designs for the preamplifier were bulkier and noisy. By making a custom state of the art preamplifier, IEM significantly reduced the noise from the signal. IEM's new preamplifier subsystem incorporated the following features:

- **Lower noise floor:** achieved by better circuit design layout and faster/lower noise op-amp devices; IEM also took into account the power supply design (see later) for its noise effects, something often neglected in other designs.
- **Faster recovery times:** Done through the gating of the signal; this permits the system to focus on only specific parts of the received pulse train.
- **Integral active filters:** for bandpass and other forms of noise elimination. In particular, IEM incorporated specialized hardware bandpass filters to eliminate specific sources of noise in the associated hardware.
- **Signal delay gating:** to simplify the analysis of the signals over time.

Results of New Preamplifier

As IEM expected, signals retrieved by the new preamplifier were noticeably "cleaner" and had spurious or irrelevant parts of the signal eliminated to a great extent. To further improve the preamp's S/N ratio, IEM redesigned it to incorporate a surface mount chip and embedded ground planes; this permitted much potential noise to be shunted off through the ground plane. This redesigned preamplifier was extremely small – measuring 1.3"x2.9" (see **Figure 13**). With these ultra-miniaturized units, IEM was able to design EMAT units that contained both transmit and receive circuitry, allowing them to operate in either mode as needed, without increasing their size; in fact, IEM's EMAT units are considerably smaller than those from our other suppliers.

Figure 13: IEM's custom designed preamp/receiver subsystem

Power Supplies

The challenges presented by the power supply have been mentioned previously. In fact, there were two power supply systems to be dealt with – a low-voltage system for the logic, preamplifier, and driver sections, and a high-voltage supply for the pulser output section; in addition, these required that a power source be selected or designed to run the supply systems that would permit the entire device to be portable. The resultant power supply systems are unique, fully custom designs. No such systems existed before this

design, as no prior EMAT systems designed were envisioned to run simultaneously at such high power and be completely portable. The design and testing of these devices involved some of the most careful design work of the entire project.

Power Supply Design

A Problem of Noise

The low-voltage supply must run the preamplifier, internal logic system, and the driver section of the EMAT. In short, it supplies the power to time the signal generation, trigger the "bang" (main pulser signal), gather the return signals, perform basic filtering and preprocessing, and send this information to the controller for analysis. The problems with this power supply stem from the fact that they are, of necessity, connected to and associated with the high-voltage supply, and the sections of the EMAT unit which the low-power supply supports are extremely sensitive to noise of all sorts. Any noticeable variation in the power supplied can produce noise. For ordinary signals this level of noise is not significant, but as noted earlier the return signals for an EMAT device are extremely weak, even with high-power pulser electronics to provide a powerful initial signal. Because of this, the power supply for the preamplifier and associated electronics must be extremely stable and low-noise, and no other sources of noise should be present, especially if they produce noise in the band for which the system is listening. However, in order to produce the signal for which you are listening, you need to use a high-power source that will generate a huge amount of noise while running, as there will be large varying currents and voltages involved. The question, then, was how to satisfy both requirements – powerful, high-voltage and inevitably noisy power supply for the pulser, and low-voltage, ultra-quiet supply for the detector and control electronics?

Solution Through Cooperative Timing

IEM recognized that there was a solution implied by the way in which the functions of the EMAT were operated. The pulser itself only needed power during the "bang" sequence. The "bang" itself, of course, was irrelevant to the detection of wheel flaws; what IEM was interested in was detecting signals ***after*** the "bang". If, then, all the "noisy" work of converting power into its proper voltage and current levels could be done during the "bang" phase, there would be an effective "quiet pause" in which the preamplifier and other low-power electronics could do their work with virtually no internal noise sources. This approach depends on extremely accurate synchronization of the electronics involved, and in rough outline proceeds in this manner:

1. **Timing driver signals** that it is time to send a pulse.
2. **High voltage supply activated**.
3. **Low-voltage capacitors charged** during high-voltage pulse preparation and generation
4. **"Bang"** sent.
5. **Timing driver signals** pulse phase is over.
6. **High-voltage supply shuts down.**
7. **Preamplifier, logic, and driver draw low-voltage current** from capacitors, providing a low-noise source and permitting the "listen" phase to pass with very little interference.
8. **"Listen" phase ends**; return to beginning of pulse phase.

While simple in basic concept, to find the precise design required took a great deal of design work and then experimentation. The end result, however, performs exactly as desired, generating virtually no noise during the crucial listening phase.

Power Source

The high voltage and current demands of the high-power supply presented another challenge. The initial power-up stage of the Portable Wheel Flaw Gauge draws considerable current, and thereafter the Gauge maintains a fairly steady draw of one ampere or so. This requires that the power source be able to provide a very high peak flow for a short time, and retain considerable capacity thereafter for long-term maintenance. Currently, IEM's solution is a customized lead-acid battery pack, similar to a miniaturized motorcycle battery. The high peak flow and reserve capacity are both common features of lead-acid batteries which has made them common choices for power sources. One drawback to this solution is that lead-acid batteries – even small ones – do not have a particularly good power density, as shown in **Table 1**. This means that a fairly large (and heavy) battery is required for IEM's application. The entire device

remains portable, but is heavier than optimal. IEM would prefer to use lithium-ion batteries, which have a far greater energy density and therefore offer the potential of a much smaller and lighter power source. However, COTS lithium batteries are not designed to safely provide the peak current draw which the Gauge requires; the charging and discharging of lithium batteries can present significant hazards if not done properly. IEM's intent for commercial development is to design a **custom** lithium-ion power source that can provide both the peak draw and the reserve capacity that is needed for this application.

Table 1: Battery Technology Survey

	Sealed Lead-Acid	*Nickel Cadmium*	*Nickel Metal Hydride*	*Lithium Ion*	*Lithium Metal*
Ave. Operating Volt. (V)	2	1.2	1.25	3.6	3
Energy Density (W-h / Kg)	35	45	55	100	140 - 300
Volumetric Eff. (W-h / Liter)	85	150	180	225	300
Cost ($ / W-h)	.25 to .50	.75 to 1.5	1.5 to 3.0	2.5 to 3.5	1.4 to 3.0
Memory Effect?	No	Yes	No	No	No
Self-Discharge Rate (% month)	5 to 10	25	20 to 25	8	1 to 2
Temp. Range (C)	0 to +50	-10 to +50	-10 to +50	-10 to +50	-40 to +150
Env. Concerns?	Yes	Yes	No	No	No

Controller

The controller (shown in **Figure 14**) is the brain of the Portable Wheel Flaw Detection Gauge. The pulser sends the basic signals; the sensor head detects the return signals; the controller's CPU and the software running thereon makes sense of these signals, stores the results, and controls all the operations of every other component of the machine. The controller integrates a number of components into a single, compact unit that contains most of the key electronics, supplies the power, supports the unit physically, and provides the user interface.

Figure 14: Portable Wheel Flaw Detection Gauge controller

CPU

IEM has designed a number of rugged datalogger and industrial computer products. Each specific application, however, has its own unique demands that require a careful re-evaluation of the current technology and a selection of an appropriate CPU – the workhorse section of the controller unit, which performs most of the work involved.

For this application, after examination of the various options available, IEM selected the ***Octagon System's 5070 CPU*** control card. This unit, intended for high-performance, low-power, rugged embedded control applications, offered a large number of attractive features for IEM's application, including (but not at all limited to) the following:

- ZF Micro ZFx86 128MHz processor (more than adequate for this application)
- Integral Compact Flash card support
- Integral LCD screen support
- Multiple OS (NT, 98, CE, Linux, DOS, etc.) support

Figure 15: Octagon Systems' 5070 CPU Control Card

The 5070 (**Figure 15**) has many other potentially useful features, including built-in connectivity for Ethernet, USB, parallel, and other interface technologies. Octagon Systems has been very responsive to inquiries and requests, and such support is always a major consideration in the design and prototyping of new products that will inevitably require support in all components if they are to be a commercial success.

Display Selection

For instrumentation applications of this nature, an LCD flat-panel display is one of the most obvious and efficient display modalities. They draw little power, have a low profile, and modern LCD panels can be quite rugged while achieving excellent resolution and providing many interface display options. For this purpose, IEM selected the Philips LB064V02-B1 LCD display. This LCD display has high

resolution color capability, a built in backlight for low-light applications, and is provided with antiglare and hard surface coatings.

In addition, this display offers one other very useful feature for this particular application. As the preferred user interface for modern applications is a GUI – graphical user interface – some form of pointing device is necessary. The LB064V02-B1 comes with an integral touchscreen capacity, eliminating the need to include a separate touchpad, trackball, or other pointing device that would add size and inconvenience.

Digitizer

The digitizer takes the analog signal produced by the preamplifier and envelope detector and converts it into a digital signal suitable for analysis by the software. There are many different digitizer cards – often called ADC (analog-to-digital converter) cards – on the market. IEM selected the Diamond-MM-32-AT card, from Diamond Systems, as the digitizer for this particular application. Shown in **Figure 16**, the MM-32-AT takes samples from the envelope at a rate of 200ksamp/sec, providing ample accuracy for detecting and locating flaws within the wheel.

Figure 16: Diamond MM-32 AT digitizer card

Power Supply

Supplying power for the CPU and associated cards required that this, too, have its own power supply. However, this section of the device did not have the same specific problems associated with the actual EMAT circuitry, and IEM therefore did not have to perform the same custom power supply design that was necessary for those prior subsystems. Instead, a low-noise, high-efficiency power supply for the main controller was assembled from two COTS components.

Integration and EMI/RFI Abatement

Having selected the components, it was then necessary to assemble all components into a functional whole. This was facilitated by having made careful consideration of integration demands early on and including those considerations in the component selection process. Because of this, integration of the physical components on a basic level proceeded smoothly; the CPU had built-in support for the display, and our design for the preamplifier and envelope detector was intended to feed directly to the selected ADC digitizer.

However, the basic assembly would not function as a unit due to other conflicts. The most important of these, on which IEM had to expend a considerable amount of time and effort, was abatement of electromagnetic/radio-frequency interference (noise). As noted previously, this problem had been dealt with on the pulser/sensing side by arranging for the preamplifier and associated electronics to be essentially inert during “bang” sequences and active in the quiet intervals. This approach, however, was not possible for the main controller, as it would effectively require a reboot of the system on every “bang”, something that would take far too long. Other parts of the system, such as the unique power systems, had a potential for similar interference.

There are basically two physical approaches that can be taken to eliminating this kind of interference: build a shield around the noisy component, or to move sensitive components as far away from the noisy one as possible. After a great deal of experimentation, IEM arrived at a final controller design that minimized noise and permitted the entire system to continue functioning reliably and swiftly. Among other required modifications, IEM designed a custom grounding enclosure for the pulser unit to intercept and contain all the extreme noise pulses from the device.

Basic Controls

Separate from the main user interface are several controls hardwired into the controller and visible on the controller’s base. **Figure 17** shows all of these connections and controls. They are:

- **Test inputs** – for verifying the functionality of the Wheel Flaw Detection Gauge. These inputs consist of a trigger signal input and a receiver for obtaining the triggered signal.

- **High Voltage Enable** – to prepare the system to actually obtain readings, the high-voltage supply must be activated. It should not be kept on at all times as this will waste power.
- **Low Voltage On/Off** – this is the main system power switch.
- **Battery Pack connection** – where the power supply connects to the controller.

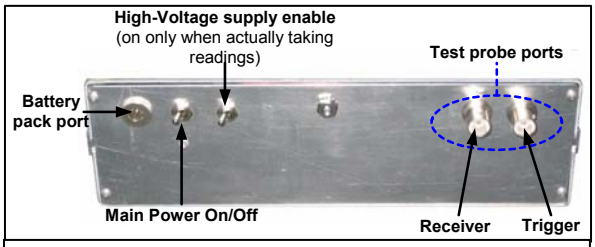

Figure 17: Hardwired controls and ports on main controller

Algorithm/Software Design and Testing

Basic Signal Processing Algorithms

IEM has performed the task of basic EMAT signal analysis many times over the years. A number of techniques have been developed that have served well in this area.

Bandpass Filtering

Ideally, a signal is sent out into the target under interrogation, and the return signal is identical to the interrogating signal except with changes that denote the flaws or structure of the target material. In the real world, however, a signal is essentially never "pure", and internal noise, outside sources of sound and electrical signals, and other elements make it likely that the received signal is not even particularly close to pure. It therefore becomes important to be able to eliminate parts of the received signal that are not associated with the interrogating pulse in which we are interested. One of the basic ways to do this is to install a filter that will not pass signals below a certain frequency or above another selected frequency; this form of filtering is called a bandpass filter. IEM has used bandpass filtering in a number of applications. **Figure 18** shows a raw wheel signal (top, showing the first, second, and third signal returns) and the signal after a bandpass filter has been applied to it (bottom). To eliminate spurious environmental and interference signals, then, IEM has installed a hardware bandpass filter.

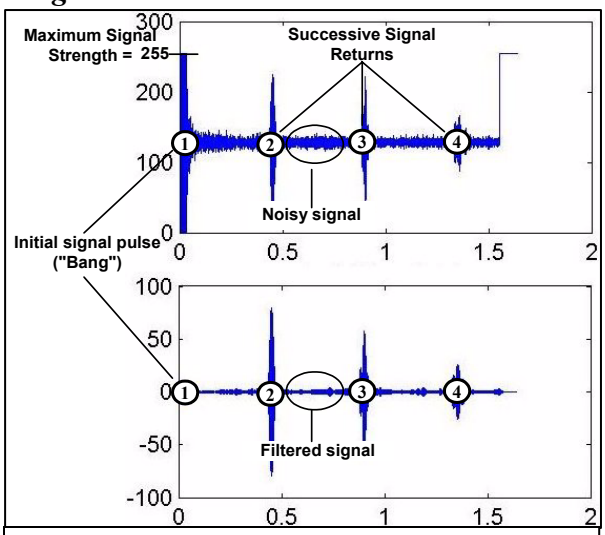

Figure 18: Bandpass filter eliminating spurious noise and leaving desired signal

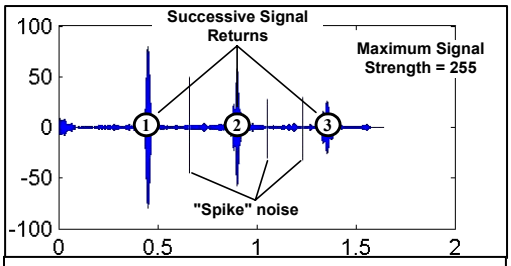

Figure 19: Bandpassed signal with "spike" noise

Noise "Spike" Elimination

In real environments encountered by IEM in the development of wheel and rail crack detection, such as train yards with large electric-based locomotives and other electrical systems present, noise "spikes" – very strong transient signals covering wide bandwidth – often are encountered. Such a signal would, after bandpass filtering, look like the one shown in **Figure 19**. To remove this type of noise, IEM uses a **dv/dt filter** – one that measures the change in overall voltage as compared with time. A true signal will exhibit some overall breadth and measurable "ramp-up" and "ramp-down"; a noise spike will go from very low to very high signal and back to low again in very short time. By eliminating drastic, very short-term changes this form of noise can be removed, as shown in **Figure 20**.

Signal Envelope Filtering

The signals above are reasonably simple to read with the unaided eye, but in order to permit automated analysis of them, they must be reduced to a curve that is better represented in ways a machine can understand. This is done by deriving the signal envelope – a curve that delineates the overall behavior of the signal. There are a number of hardware and software methods for doing this; for purposes of the portable Wheel Flaw Detection Gauge, a hardware solution is preferred, as this saves on processing demands in the restricted processing environment of a portable device. In simplified terms, the signal envelope is derived by taking the original signal, converting the negative portions of the signal to positives and adding them to the positive portion of the signal, and then producing a curve that outlines, or "envelops" the resulting signal graph. The resulting envelope is smoothed to produce an actual curve. This process is represented visually in **Figure 21.** Note that **Figure 21** is done on different data than the prior figures, to show some more features; a flaw signal can be seen between the returns.

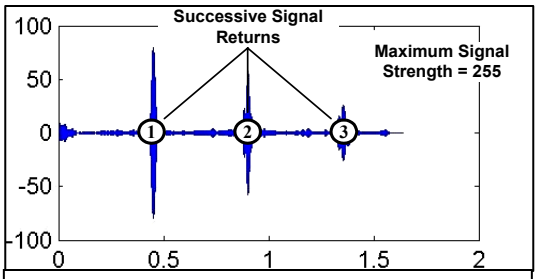

Figure 20: Noise eliminated from signal after dv/dt filtering

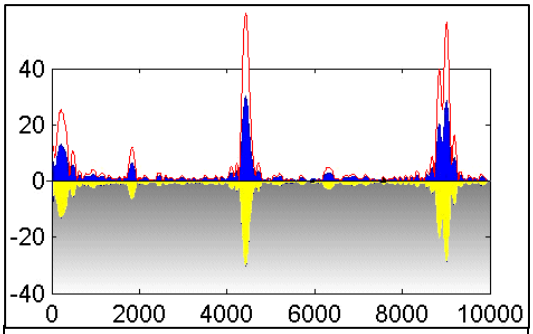

Figure 21: Signal Envelope

Signal Averaging

As signals in field conditions tend to be relatively "rough", even after the previously-described approaches to improve the signal, IEM utilizes a ***rolling*** average in approach to "smooth" the signal. This can eliminate spurious signal spikes and produces curves that are more amenable to mathematical analysis; this is very important for automating the analysis of wheel data. In this case, we are averaging the value of a group of XY values for a given period of time – points 1, 2, 3 are averaged, for instance, and then points 2, 3, and 4, and so on. As the number of points increases, there is a growing apparent time-shift delay in the resultant curve (due to the points being the average of data that is slightly displaced in time relative to the "original"), as seen in **Figure 22**, which shows a set of regular time-domain data and the result of a 100-point rolling average of this same data. Note that the average data is smoother, much of the noise cancelled out, but that there is a delay in the peaks derived from the point averaging. In order to line the peaks up, an automatic time-compensation function must be applied. We apply just such a function in **Figure 23**, showing that the clarified curve is now properly aligned with the raw data. **Figure 24** shows this process applied to the signal envelope **(A)** derived from **Figure 20**, the result visible as **(B)**. A comparison of the two images shows that the signals have been emphasized and their transitions smoothed.

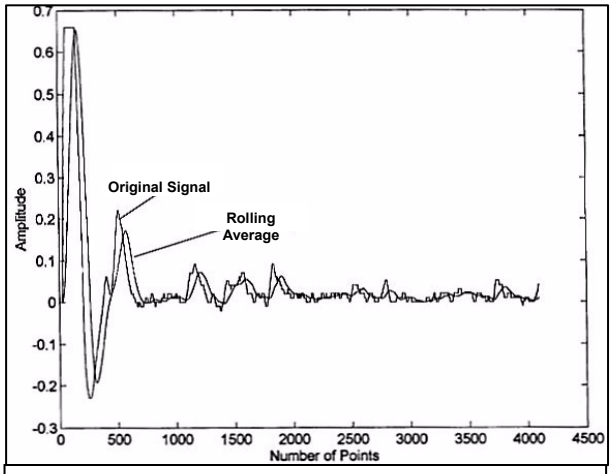

Figure 22: Rolling Average, non-time-compensated

Advanced Algorithms

Feature Extraction and Thresholding

In order to provide a device that performs most of the work for the user, it is necessary that the Wheel Flaw Detection Gauge be able to actually determine the existence of flaws on its own. One necessary component of this is to enable the device to be able to tell when "peaks" (significantly higher

periods of signal) occur within the signal, and whether those peaks exceed some level of signal that would indicate that they were true detected signals rather than just artifact of noise. The first of these subtasks involves feature detection and extraction; the second, the establishment of a threshold and the detection of anything that surpasses that threshold. These are examples of tasks that are essentially trivial for human beings because we have built-in feature extraction and threshold detection ability; it is, therefore, common for people to underestimate the difficulty of these tasks in the computing world. In actuality, developing such algorithms is a very nontrivial task if the results are to be robust and reliable.

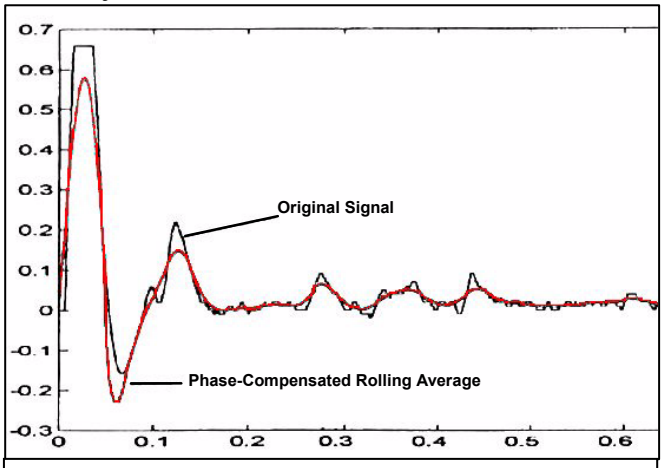

Figure 23: Time-phase compensated rolling average

Figure 25 shows IEM's feature extraction and thresholding algorithms applied to the signal envelope generated in **Figure 24**. As can be seen, these algorithms establish several thresholds – two for the detection of the return of the main signal, suitably scaled for attenuation over space and time, and two in the corresponding intervals for detecting potential signals within those intervals; these pairs are the higher and lower generally horizontal lines seen in **Figure 25**. Each detected feature within the critical intervals is shown by an asterisk; as can be seen, IEM's algorithm detects every notable peak within the intervals.

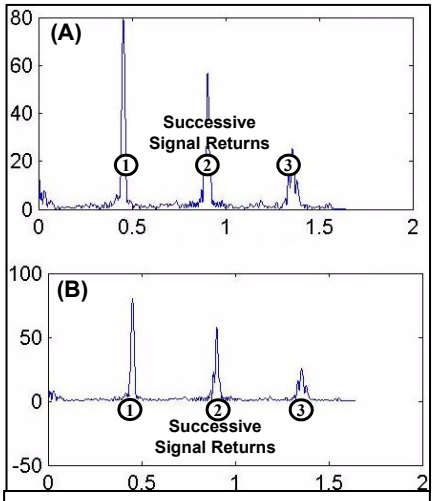

Figure 24: Rolling average applied to signal envelope

Expert System

An "expert system" is one of several types of so-called "artificial intelligence" utilized in "smart" electronic systems. Others include fuzzy logic systems and Artificial Neural Networks (ANNs), both of which IEM has used in other applications.

Expert systems are essentially collections of rules and decision trees that enable a system to perform a function very similar to that performed by an expert in the field in question. As a simple example, if you wanted to program a shopping robot to evaluate produce so that it would always get vegetables of appropriate ripeness and condition, the part of the expert system associated with, say, choosing the right avocados for making guacamole might involve rules about determining the state of an avocado, first via visual cues (how green, holes or clearly rotting spots, etc) and then by tactile examination (how firm or soft the avocado is), and then make decisions about the acceptability of the avocado based on the results of these rule inputs.

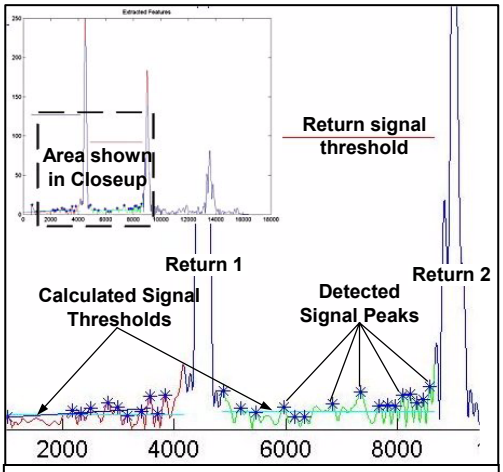

Figure 25: Results of IEM's feature extraction and thresholding algorithms

To create the current expert system for the Wheel Flaw Detection Gauge, IEM tested a number of different wheels in various circumstances and monitored the process by which we were able to determine the presence or absence of flaws, their nature, and so on. The results of this monitored process were codified into a rule-decision set that represented the evaluation, selection, and decision

process of IEM's experts on the use of EMAT technology. After primary evaluation of the expert system, IEM decided to incorporate additional programming in the form of fuzzy logic decision-making software, creating a "Fuzzy Expert System".

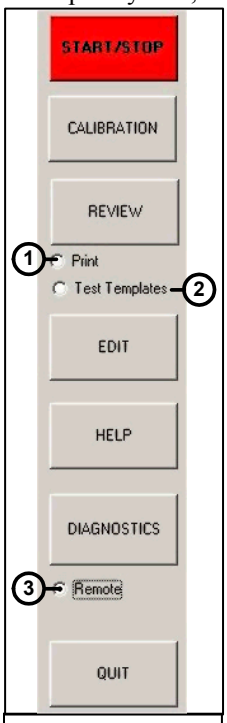

Figure 26: Controls for the GUI

Graphical User Interface (GUI) and Typical Use Procedure

Overview

Separate from the data processing software, the Graphical User Interface (GUI) facilitates the interaction of the user and the instrument by making it simple to control. IEM has prototyped and tested an appropriate GUI for the Wheel Flaw Detection Gauge that offers all of the basic functions for control of the Gauge functions and the display and storage of results. The control panel for the GUI can be seen in **Figure 29**. Following a discussion of the controls of the GUI is a brief description of the procedures followed when using the Portable Wheel Flaw Detection Gauge.

Main Control Descriptions

The main GUI screen offers seven main control choices, labeled **Start/Stop**, **Calibration**, **Review**, **Edit**, **Help, Diagnostics**, and **Quit**, as shown in **Figure 26**. While they may seem self-explanatory, a quick description of each is in order. Supplemental radio buttons are labeled in **Figure 26** and discussed in their appropriate section.

Start/Stop

As might be expected, this is the control used to begin and end sessions of data recording/analysis. In the prototype, this can be set to utilize single data files for demonstration purposes, or a larger test data file. **Figure 27** shows the GUI after running a test on a good wheel. Once the system is started, it will obtain a reading, displaying the raw data in the left-hand window (this data can be shown as the raw pulse-echo or as the signal envelope) and the threshold/feature analysis graphs (of the sort originally shown in **Figure 25**) in the right-hand window. The bottom window displays the results of the expert system in judging the condition of the wheel. The system attempts to present the data in all three formats to allow the user to have the most clear and complete view of the behavior of the data. For standard inspection purposes, of course, the key data will be contained in the bottom window: the determination of whether or not the wheel is good or bad. The determination of whether a wheel is good or bad, and, if bad, what the condition in question is, is done by the expert system. Selecting the "Print" radio button (#**1** in **Figure 26**) prints the results of a scan.

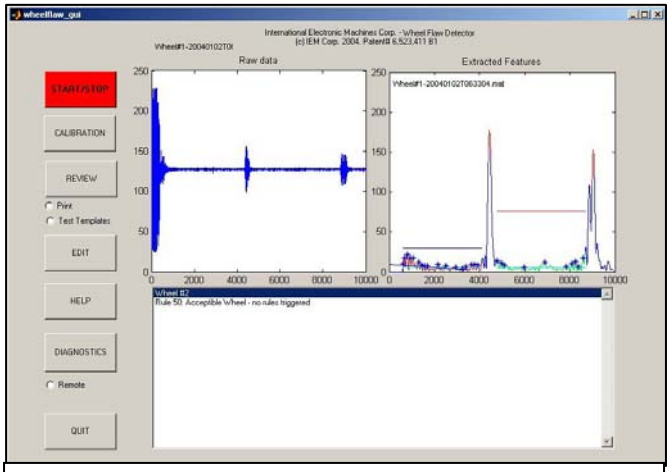

Figure 27: Wheel Flaw Detection Gauge GUI showing the capture and analysis of a good wheel.

Calibration

Selecting **Calibrate** prepares the system for calibration and testing. This procedure must be done immediately before the system is first used, so as to ensure that it is functioning properly and to adjust for the specific design parameters for each individual system. Following this, calibration will be needed only infrequently, either as part of specific periodic maintenance procedures, or under circumstances in which the user has reason to suspect some problem with calibration due to unusual readings or an accident or other event that may have affected the system.

In order to properly calibrate the system, the user must make sure that the proper **calibration wheel** is available. This calibration wheel has been engineered by IEM to produce signals that emulate those of specific flaws, thereby allowing the detection and expert system to be directly tested and adjusted. When Calibrate is selected, it will remind the user that a wheel must be selected and the Wheel Flaw Detection Gauge's sensor had placed upon the calibration wheel. This message is shown in **Figure 28**. Click "OK" after ensuring that the sensor is correctly placed; if it is not, calibration cannot occur and the user will see only error messages.

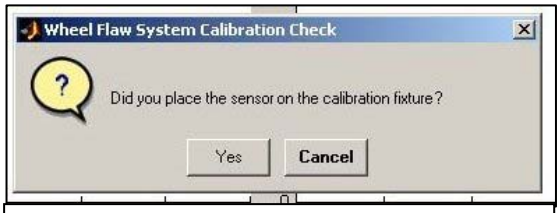

Figure 28: Popup window asking user to verify the sensor is on the calibration fixture

Calibration only needs to be done under two circumstances: firstly if the sensor head is changed (as each head will have its own detection characteristics) and secondly if the user notes behavior that indicates that the unit is not well calibrated. It may be of use, however, to follow procedure similar to that used with IEM's Portable Electronic Wheel Gauge, and check calibration at the start and end of each shift, simply to ensure the procedure is never entirely forgotten. Checking calibration is very quick, a matter of a minute or so.

Review

Review is used for checking prior results, comparing old data with new, and so on. Upon selecting Review, the user is presented with a choice to select the file containing the data that he or she wishes to review. Once the file has been selected, it is analyzed and displayed just as though it were new data (as shown under the "**Start/Stop**" section). Associated with the Review function is another radio-button style control (#**2** in **Figure 26**) called "Test Templates". This permits the user to utilize signal template files supplied with the system (see **Prototype and Field Testing** for more detail on these files).

Edit

The "Edit" choice opens a file menu that permits the user to examine and edit specific system files to meet their specifications.

There are currently three system files relevant to the Edit GUI selection. These three files are:

- **wheelflaw-default.sys –** this file stores all of the control values for running the wheel crack detection application, including the sampling frequency, number of samples, flag values for what actions the program takes at various points, and so on.
- **wheelflaw-logfile.sys –** this file records all the activity of the wheel crack application, unless the controlling flag variable in d**efault.sys** is set to disable this.
- **wheelflaw-rules.sys –** this file contains many of the rules used by the expert system to determine what wheels are and are not bad. Having this available as a separate file greatly facilitates the fine-tuning and upgrading of the expert system.

Help

Selecting the **Help** button will bring up the **Help** files, including the User Manual, for the Wheel Flaw Detection Gauge.

Diagnostics

Any instrument can develop difficulties, due to external or internal factors. Thus it is necessary to provide means to analyze the functioning of the device and determine what may be going wrong. A number of different responses or choices may be available during a diagnostic run.

If the main unit is connected to the Internet in some fashion, the radio button seen in **Figure 26** labeled as #**3** ("Remote") may be selected. If it is active, the Wheel Flaw Detection Gauge will be able to communicate with IEM directly, and IEM can diagnose, troubleshoot, and often will be able to fix any issues remotely from our headquarters.

Quit

This selection needs little explanation. When **Quit** is clicked, the wheel crack application shuts down. Remember to save any data before quitting, or it may be lost.

Using the Portable Wheel Flaw Detection Gauge

The procedure to use the Portable Wheel Flaw Detection Gauge is fairly obvious and straightforward. The following list gives the procedure steps and approximate time.

1. **Activate Gauge.** The Gauge is first activated by turning the main power switch (see Figure 17) to "on". This will cause the machine to "boot" and will automatically load the testing application. This will take a minute or two. The Gauge can be left on subsequent to this, so this time cost applies only once per "shift" of use.
2. **Sign In.** The user will be given some sort of designation (username and password, etc) so as to track and control use of the system. This takes about 10 – 15 seconds and is also a once-per-shift task.
3. **Enter Pre-measurement data.** This may include things such as the train car designation, specifics of the type of testing being done, and so on. This is a bit hard to estimate as there could be automated methods for doing this in some settings (and thus once the measurements begin there is effectively no time cost), or there might be several entries needed. Done once per each vehicle, and may take 30 seconds or so; the user then readies the Gauge by selecting the "Start" button from the user interface.
4. **Remove coverplate.** This has to be done just before starting a sequence of readings; **2 – 5 seconds**.
5. **Take measurements.** The user places the sensor head on the wheel, activates the high-power switch (**Figure 17**) to permit it to take a reading, moves the head (as discussed in **Usability Issues**) if desired for a second reading, and then switches off the high power and removes the sensor head; if care is taken the coverplate may be left off until all readings have been taken, but if any significant interval is to pass between readings the coverplate should be reapplied. This sequence takes 20 seconds or less to complete; a strong, fast user could conceivably perform two readings on one wheel in 5 seconds. The user then continues the procedure until done with all wheels on that particular vehicle, at which point they would select the "Stop" command on the user interface and repeat steps 3 through 5. Remember to reapply the coverplate if any significant interval is to elapse between measurements.

The other described options in the control interface will generally be used in an office setting – reviewing prior data, calibration, and so on. The precise nature of the entry and use procedures will need to be determined and is discussed in the **Needed Refinement for Commercialization** section.

Usability Issues

Mechanical Support Components

Due to its "front-line" position in the wheel evaluation, the sensor head must be made as rugged as possible, despite the presence of delicate interior components. The rugged and solid nature of the head is best seen in the rear view shown in **Figure 29**; the main casing is solid metal and able to withstand a great deal of punishment.

Figure 29: Sensor Head rugged metal housing

The PEEK plastic that protects the coils has demonstrated excellent wear resistance; however, it is not particularly resistant to punctures from sharp or edged objects pressed against its surface. Unfortunately, with a magnet of the strength needed to perform the EMAT readings, steel objects such as screwdrivers, loose screws, and metal debris, if present, can be drawn to the coil region by the magnet; the impact and attempts to remove them can easily damage the coil through puncturing or cutting the PEEK casing. To protect the coils when readings are not being taken, a steel coverplate was fashioned. The EMAT magnet holds the coverplate firmly on; removing the flat coverplate is difficult, so IEM is

experimenting with a number of potential designs for removing the plate more easily. Figure 30 shows the coverplate in position on the sensor head.

Figure 30: Sensor head with protective coverplate

Figure 31 shows the sensor head with the coverplate removed; the coils are clearly visible through their casing. It is strongly recommended that the coverplate only be removed when readings are about to be taken, and replaced whenever a series of readings have been finished; this minimizes the chance of accidents as described. When the cover is off, basic precautions should be taken, such as ensuring no sharp/edged metal tools or other objects are in the immediate vicinity, and performing a quick wipe (with a rag, rough cloth, etc.) of the wheel surface to ensure no sharp pebbles, metal shavings, or other edged materials are present when the head is placed on the wheel.

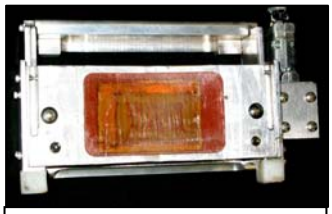

Figure 31: Sensor head without protective cover

Figure 31 also illustrates one of the other unusual features of the sensor head – the mechanical design necessary to enable users to remove the sensor from the wheels it is examining. As shown previously in **Figure 10**, a pair of plungers, activated by squeezing a handle on the sensor head unit, is included in the sensor head design to assist in overcoming the powerful pull of the head's magnet, that would otherwise make it extremely difficult to remove. The operation of this mechanism is shown in **Figure 32**, though with the head turned upside down to show how the head is removed. In actual operation, the coil side of the sensor head would be resting on a wheel surface prior to removal.

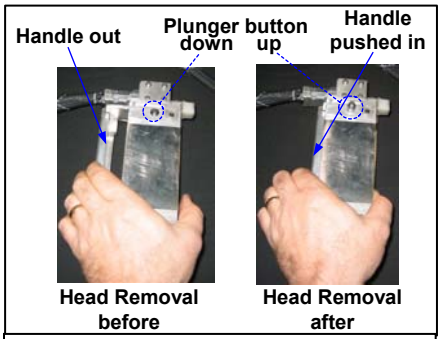

Figure 32: Operation of removal assisting plunger mechanism

The user grasps the sensor head firmly, and then squeezes the handle. This has a cam-based lever action on the plungers, that are forced up and out of their settings and push the head away from the wheel. The user then pulls up and away with a slight twisting motion, removing the sensor head from the wheel with ease; without using the plunger-based removal system, it is possible that a smaller or weaker user would find it virtually impossible to remove the sensor head at all!

Prototype Field Testing

Using the components discussed previously, IEM assembled and field tested a prototype of the Wheel Flaw Detection Gauge. This prototype is shown in **Figure 33**, and consists of the sensor head and connector, main controller, and power pack (on back of unit).

Figure 33: Prototype of Wheel Flaw Detection Gauge

Tread Flaw Field Testing

Field testing of the device used the collection of wheel sets IEM has for our in-house railroad testbed (a total of 8 separate wheel sets). These sets include wheels with known flaws, new wheels, and used but still good wheels. Some of these wheels were shown in **Figure 2**, illustrating some of the flaws for detection. One of the wheels (**Figure 2D**) had a small crack machined into it, as it is difficult to locate an actual wheel that has an adequately small flaw of this nature for testing purposes. The machined crack was 65mm (2.56 inches) long, running across the tread towards the field side, and had a depth and width of 0.8mm (0.0315) inches, making it a quite subtle defect in terms of size. Another similar crack was later machined into one of the known-flawed wheels to provide two separate flaw targets in a single wheel for testing. All of the flaws in IEM's test wheels were visible on the surface. Broader testing should be done on known-flawed wheels at some

location such as the TTCI that has many such sample wheels, including some with subsurface flaws not externally visible.

In addition, IEM extracted EMAT signal data for wheels from a wayside crack detection system developed by the U. S. Department of Transportation and AAR. This system used similar techniques for analyzing wheel flaws (Robert K. Larson Jr., Robert L. Florom, and Britto R. Rajkumar, *Field Testing of a Wayside Wheel Crack Detection System*, U.S. Department of Transportation, Federal Railroad Administration, Office of Research and Development; DOT/FRA/ORD-92/07, Final Report, May 1992). IEM used their initial signal graphs, extracted the data therefrom, and constructed input signals from them that corresponded with the signals such wheels would have given our system. These signals were then presented to the Gauge for analysis. This gave IEM data from 20 additional wheel sets. These signals were especially useful for testing our Fuzzy Expert System and are made available by the system under the "Test Templates" option in the GUI, providing sample signals for a variety of wheels and flaws.

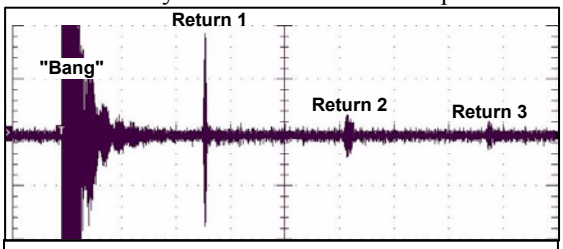

Figure 34: Raw data returns from new wheel

Figure 34 shows the bang and returns from a new wheel. Note, again, that this is ***raw data*** – no processing at all. Nonetheless, three returns can be seen clearly. After processing, IEM could see four returns from new or like-new wheels routinely.

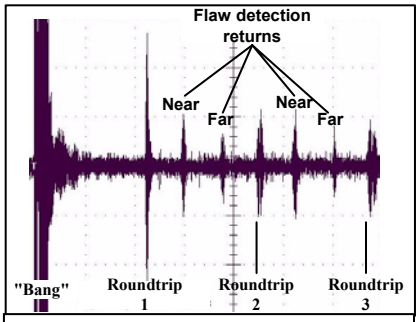

Figure 35: Detection of small crack in raw data

The raw data return from a flawed wheel – in this case, the one with the small machined crack of a depth of less than 1mm – is equally illuminating. Shown in **Figure 35**, it is clear, even to the naked eye, that the flaw is visible to the instrument and the system easily distinguishes the existence and location of the flaw.

Measurement Procedures and Statistical Results

Measurement Procedures

The following discussion focuses on the image seen in **Figure 36**, which is another actual test wheel from IEM's work. The image shows the main "bang" (far left) and two roundtrip return signals, with a flaw signal present between the roundtrip signals. It was first necessary to determine in the field the actual speed of the acoustic signal in railway wheels. Multiple tests on our in-house wheels were done to determine this; for instance, on a 33.05" diameter wheel (with, therefore, a circumference of 103.83"), it took an average of 876 microseconds (µs) for the signal to complete a full roundtrip. Dividing the distance by the number of inches yields us the speed (inches/µs) of the signal, which is 0.118in/µs. This velocity measurement was consistent to within the limits of our measurement (physical ability to measure location of receiving sensor on wheel, etc.) across all wheels tested, new, old, flawed, and unflawed.

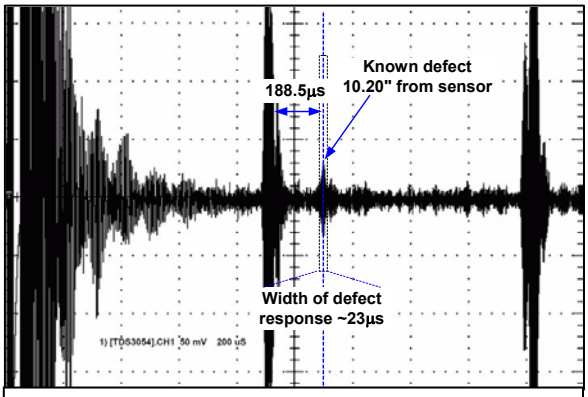

Figure 36: Example flaw detection graph for discussion of measurement technique

As measuring the distance to a flaw depends on the time from the initial signal to the return from the flaw, the width of the flaw response is the major constraint on the accuracy of the measurement. In testing the flawed wheels in our in-house collection, we measured the width of the flaw response to

determine this constraint. On average, the flaw response is approximately 23μs wide, which combined with the previously determined velocity yields a return pulse width of approximately 2.7 inches; this means that any measurement obtained is only correct within ±1.35". As the wheels are typically something around 100 inches in circumference (anywhere from 87 [28 inch wheels] to over 130 [42 inch wheels]), this is an error of between 1 and 1.5%. This "window" is shown in outline in Figure 39. In this figure, a known defect (the machined crack described earlier) is physically measured to be 10.2" from the sensor head. When the Gauge is activated, the return pulse from the flaw is seen 188.5μs after the main pulse. Multiplying by the pulse velocity yields a return distance of 22.243"; however, this is actually twice the distance to the flaw as seen by the gauge, since the time involved is the time for the signal to travel to the flaw and "bounce back", returning along the same path. Thus, the distance from the flaw according to the gauge is 11.12" from the sensor, a discrepancy of 0.92".

Statistical Results of Gauge Tests

IEM took multiple readings on all 8 non-flawed and flawed wheel sets in our collection with the sensor head placed at three or more different positions around each wheel. In addition, we took multiple readings (at least three) with sensors in the same location, to verify that the Gauge would produce the same results upon repetition. Repeating the reading procedure at the same location produced results that could not be discriminated from each other by any reliable method; whatever margin of error exists within the Gauge itself is smaller than the error introduced by external factors such as the limits of physically measuring a path along a wheel. The flaws available in our wheel sets included condemnable shelling, cracks (machined), hollow tread, and gouges/dings.

It was possible to determine the statistical variance for the measurement distances as determined by the Gauge to the flaws on various wheels. As it turns out, the above example's discrepancy of 0.92" is the largest discrepancy seen in IEM's testing regimen. Overall, including all tests on our 8 in-house wheel sets as performed multiple times by different operators, the standard deviation of measurements was shown to be 0.5221 inches. Assuming a standard bell-curve distribution for error, this means that 95% of all readings would be expected to be within 1.044 inches of the true value; by comparison with the pulse-width gap determined earlier, it can be seen that the accuracy of the Gauge is in fact determined by the limitations on the physical pulse return itself, as the pulse width covers more than 2.5 standard deviations. The following summarizes the results from our field tests of the prototype:

- **The prototype is consistent.** It gave the same results for every wheel set under repeated readings.
- **The prototype is reliable.** It never rejected a good wheel, nor passed a bad wheel.
- **The prototype is accurate.** Whenever it diagnosed a flaw or fault, the wheel in question did indeed have the flaw or fault in question, and the fault or flaw was to be found at or very near to the location indicated by the system.
- **Failure of the prototype to acquire data when properly placed only occurs when the wheel itself is bad.** Only shelling of a condemnable level (as defined in the AAR manual -- ***Why Made code 75***) or very severe hollow tread (necessitating wheel turning) caused sufficient loss of signal to prevent a reading; spalling, moderate shelling, grease, paint, and other contaminants had no effect on the function of the device.
- **The prototype is fast.** To obtain two separate readings of one wheel, in two locations, takes less than 20 seconds.

The field tests on real wheels demonstrated that moderately hollow tread presented some minor contact difficulties; IEM has already designed a new contact head that eliminates this difficulty while remaining able to contact non-hollow tread. Other than this, no major problems were encountered throughout all of the live testing of the system. These tests focused on our initial sensor head design, for tread flaw detection. Towards the end of the development cycle, IEM tested the system using a new head for detecting flange flaws.

Flange Flaw Detection Field Testing

For simplicity in experimental design, IEM utilized a dual EMAT, one transmitting and one receiving (AKA the "pitch-catch" configuration), for the flange flaw detection head; this also allowed us to test different physical EMAT configurations for their efficacy in this application. A sample of the raw signal graph returned from this configuration is shown in **Figure 37.**

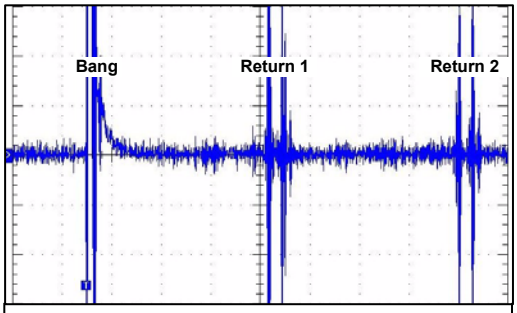

Figure 37: Return raw signal from pitch-catch EMAT on Flange

One clear difference between this and the prior configuration is the double-peaked shape of the "bang" and subsequent returns. This derives from the fact that there are two closely-spaced transceivers on the sensor head, and thus the device receives two closely-spaced signal spikes whenever the signal passes the head.

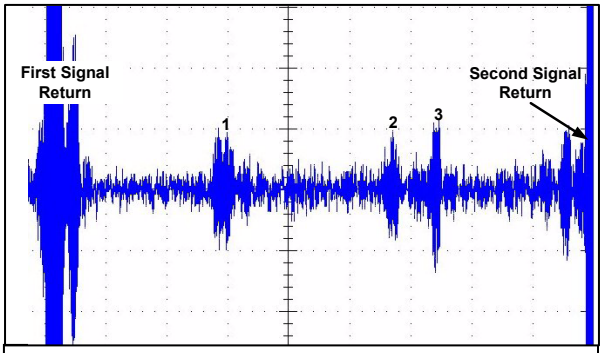

Figure 38: Flange signal showing flaws on flange

This configuration demonstrated the ability of our system to detect flange-related flaws, as shown by the averaging and enlarging of several signals such as the one shown previously. **Figure 38** shows the resultant graph, focused on the section between the first and second return signals. Indications of flaws are indicated at points 1, 2, and 3; #2, in fact, is a secondary echo of #1 (as seen for the prior flawed wheel signals depicted in **Figure 35**), but #3 indicates a separate flaw. In fact, this wheel does indeed have small defects on the flange area (dings and a small cut on the edge), in the locations indicated by the return signals. Similar tests on IEM's other in-house wheels yielded results consistent with those seen with the tread flaw sensor head: good wheels were passed, bad wheels were not, and the system had an extremely low false positive and false negative rate.

Conclusions

IEM has constructed a portable Wheel Flaw Detection Gauge. This device can be applied to the tread at two points (which need be separated only by a short distance) in a matter of a few seconds, and from these two quick readings determine if flaws exist within the wheel, and if they are present the number, size, and nature of these flaws along the tread. IEM has further demonstrated that it is eminently possible to perform the same function for other portions of the wheel, using a device that differs from the tread flaw detection configuration only in the "sensor head" used to deliver and receive the EMAT signals.

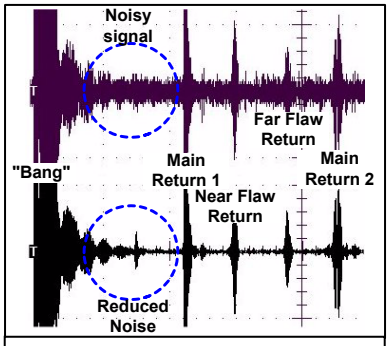

Figure 39: Raw and averaged signals from machined crack

One major and important difference between the portable and rail-based versions of this technology stems from the time element involved. An on-rail system, checking wheels as they pass, is severely limited in its detection ability by the fact that it will have only one chance of short duration to examine the wheel. A failure in coupling will result in no wheel reading, and even with good coupling only a few pulses can be successfully sent. The limiting factor for wheels in such a setting is that the wheel must remain in contact with the sensor head for at least the duration of one, and preferably two or more, roundtrips of the signal around the wheel – a duration of slightly over one millisecond. Even a relatively slow-moving train does not provide many chances for such a reading on a stationary, rail-based system, as the length of contact is approximately one inch.

The Portable Wheel Flaw Detection Gauge, being hand-operated on a stationary wheel, can and does obtain multiple cycles of data routinely. This results in the ability of the portable device to provide higher-quality, more accurate results. A simple example of how this is accomplished is shown in Figure 39 at the top we have a single raw signal from the cracked wheel shown in Figure 35, while at the bottom is an averaged signal, using 16 separate readings averaged into one.

The bottom version is clearly superior, sharper, with more clearly defined peaks and much diminished noise, as discussed earlier in the sections on signal processing. Note how even at the very beginning of the signal, following the "bang" – when there is much unavoidable noise and the signal tends, therefore, to be useless – the noise has been drastically reduced and in fact the flaw return signals are becoming visible, even with this very elementary process. Such additional data refinement has a "cascade" effect; by being able to use simple means to dramatically improve the basic signal, the other more advanced signal processing methods become capable of producing even more impressive results themselves, locating and defining flaws and features that would be otherwise indistinguishable. These 16 separate readings were obtained in approximately half a second – incurring no delay for the operator. For an in-ground system, however, such time would be an unaffordable luxury – it is the equivalent of a train moving at less than 1.5 miles per hour. Thus, in-ground or on-rail systems will likely be best used as screening devices – passing clearly good wheels through and sending any questionables to be examined by a portable device such as this one, that will be able to quickly determine the nature and extent of any flaws in a wheel.

The Portable Wheel Flaw Detection Gauge has met or exceeded most of IEM's original design requirements, as shown in Table 2.

Table 2: Requirements and Performance of Wheel Flaw Detection Gauge Prototype

Mechanical Requirement Specifications			
Category	**Requirement**	**Required or Preferred**	**Status of Requirement in Prototype**
Size	As small as practical; will contain a keyboard-style datalogger, so will not be overly small	*Preferred*	13"x8"x3" main unit. Can be made somewhat smaller for production version
Weight	5 - 10 lbs or less if possible. Based on IEM experience in prior portable design (Portable Electronic Wheel Gauge, etc)	*Required*	7 lbs main unit, 3 lbs sensor head -- 10 pounds plus batteries (6 lbs lead-acid; 3 for lithium-ion). Additional lightening for production version
Application	One handed application/removal from wheel	*Required*	Yes
Maximum 'G' force	100G for short durations as shock. Non-repetitive, damping sinusoid. All three axes. Necessary for dealing with hard use in train yards -- drops, impacts, etc.	*Required*	Yes
Vibration	Large amplitude vibrations at <50Hz frequencies prevalent in off road vehicles with poor suspensions. All three axes. Typical level at 20G for up to 200msec. Basically assumes that gauge may be transported casually via vehicle over sometimes rough terrain.	*Required*	Yes
Environmental Requirement Specifications			
Category	**Requirement**	**Required or Preferred**	**Status of Requirement in Prototype**
Temperature	-25F to 125F	*Required*	Yes
Humidity	95% non-condensing	*Required*	Yes
Pressure	Altitude - 15000 feet	*Preferred*	Yes
Precipitation	2" / hour. Waterproofing required	*Required*	Will function in rain; waterproof
dirt/ dust/ grease	Must not affect operation	*Required*	No effect from grease/dirt/grime on unit
paint/ shelling/ burned on grease	Must penetrate at least 1/16" of interfering surface coatings or conditions.	*Required*	Can penetrate over 1/16" of paint, non-condemnable shelling, and other coatings

Wheel Flaw Detection Requirement Specifications			
Category	**Requirement**	**Required or Preferred**	**Status of Requirement in Prototype**
Flaw types to be detected	Thermal crack; damaged tread (not flat); slots, other cracks, or gouges.	*Required*	Yes
Flaw Locations	tread or flange	*Required*	Tread fully functional. Flange demonstrated and prototype sensor head created. Needs swappable connector for multiple head designs
	rim or plate	*Preferred*	Head designs for rim and plate examination being created. Modeling demonstrates such sensor heads are practical
Min detectable flaw size	5% cross section, or 0.25 inches, whichever is smaller	*Objective*	Yes; Demonstrated detection of flaw depths and widths measured in millimeters.
Maximum time for detection	~2 sec or less	*Required*	Yes (less than one second)
Readings per wheel	no more than 2	*Required*	Yes. 1 or two readings at most needed
User Interface			
Category	**Requirement**	**Required or Preferred**	**Status of Requirement in Prototype**
Size	one handed use; small screen	*Required*	Main unit shoulder, one hand sensor placement
Display interface	single small text screen showing status, readings, additional information	*Required*	Can also show small graphics and other information as desired
Color or Mono	Color	*Required*	Yes
Display style	hand-carried controller unit, LCD screen with light for dark conditions	*Required*	Yes
Display Control	Change font style/size for preferred viewing parameters	*Required*	Yes
Data Displayed	Gauge status (on/ready, low power, reading, error), reading results (flaw found/ estimated location/size, no flaws, error)	*Required*	Yes
Setup Time	No more than a few (5) minutes from cold startup. Effectively no prep time for taking measurements afterward.	*Required*	After practice, takes 4 minutes or less to bring system to full readiness and begin taking readings.
Measurement Time	One minute or less to obtain a reading when system is prepared and running.	*Required*	20 seconds
Takedown Time	No more than 5 minutes to shut down and put away.	*Required*	Takes less time than set-up time
Miscellaneous			
Category	**Requirement**	**Required or Preferred**	**Status of Requirement in Prototype**
Price	~$12,000 per unit	*Preferred*	yes
Batteries	Endurance (longer life better)	*Preferred*	Lead/acid batteries 2.5-3 hours; with lithium battery pack, 6 hours
	Size/weight (smaller better)	*Preferred*	Lead/acid pack measures 6 lbs; lithium battery pack would be half the size and weight
Calibration Wheel	Provides reliable verification of operation of device and flaw detection/classification rules. Small enough to keep in office or shop area.	*Required*	Yes. Calibration wheel is carryable, has reference flaws for calibration, calibration need only be done periodically to verify functioning of gauge
Modularity	wearable parts should be easily replaceable	*Preferred*	Yes

Needed Refinement for Commercialization

The prototype as designed should have several additional refinements done in order to transform it into a full-production commercial product. The current fully-functional prototype only detects flaws on the tread of the wheel, although the sensor head for detecting flange flaws has been tested, and another head for detecting flaws in the rim is under development. These refinements, as IEM currently sees them, are described below, and would be the natural subject of Phase II development.

Hardware Refinement

During the prototype stage, it is generally preferable to leave at least some extra space or "wiggle room" in the physical design to allow for the work done in adjusting components, testing new

configurations, etc. In the final design, IEM will reduce the space of components and optimize physical configurations to present the most compact design that is consistent with maintaining high performance. To be able to detect flaws in other parts of a wheel such as the flange or rim, as mentioned earlier, IEM expects that different sensor heads would be needed to properly adhere to and induce signal into the wheel; this is due to the fact that the type of ultrasonic wave needed (Lamb, Reynolds, etc.) and angle of induction depends on the type of flaw and the location being probed, and these are produced by different head designs. IEM therefore would, after determining proper design for the different heads, create a sensor head design that would permit simple and fast switching of the sensor heads, preferably one-handed. In addition, a slight redesign of the head to permit for some curvature of the tread surface is already underway to permit coupling with moderately hollow tread. In order to minimize both size and weight, IEM will also need to design a custom battery pack using lithium-ion technology. As Table 1 shows, the far greater energy density of the lithium batteries will permit a much smaller battery pack to be designed once a method has been devised to safely permit the pack to provide sufficient peak power. Ergonomic design considerations must also be taken into account (see Final Remarks and Last Minute Results). This includes designs for removing the coverplate (several being tested), for carrying the gauge and controller, displays, and so on.

Software Refinement

Besides refining the software, and optimizing it for performance, IEM will examine the feasibility and desirability of adding other options to the analysis software, such as multiple-signal averaging, frequency spectral analysis, and possibly more advanced approaches such as a version of our signal detection algorithm developed with the Department of Defense. Additional work will also have to be done on customizing and optimizing the user interface to present the most useful and attractive set of features and performance. This will be done as part of an extensive set of field usability trials, where IEM will obtain additional input from various users as to the needed/desired features of the system and incorporate these results into the final design.

The calibration procedure, discussed earlier under the User Interface, must be explicitly codified, and made an integral part of the system maintenance procedures. As currently designed, calibration is only necessary when changing sensor heads or if the user notes some discrepancy that indicates a mis-calibration. IEM has not seen a case in which the system lost calibration on its own; this does raise the problem that if no set routine is determined for calibration, the system may never be calibrated. Thus the system must be supplied with an option which will remind the user to calibrate whenever some interval passes. The software for all functions must be compiled and placed in firmware onboard the Wheel Flaw Detection Gauge. The full set of support documentation (Help files, maintenance and use manuals, etc.) must be written and included with the finished product.

Final Remarks and Last-Minute Results

IEM has demonstrated that the Portable Wheel Flaw Detection Gauge can be configured to not only detect flaws on the tread, but on all other parts – the flange, rim, and hub – of train wheels; TTCI has confirmed that tread, flange, and rim flaws are of interest and importance to freight rail. It has been specifically demonstrated that even very small flaws produce clear and unambiguous signals and that different types of flaws produce different characteristic signals. This permits the Gauge to not only determine that a wheel is flawed, but to determine the size, location, and specific type of flaw detected.

Subsequent to the completion of this project, IEM has performed some usability tests with in-house and visiting personnel from various railroad organizations, including CSX. Consensus at this time is that the “phone book” sized controller box may be better configured as a “lunch box” style device. IEM has also begun development of an ergonomic/usability testing program with input from TTCI that would be able to be combined with direct demonstration and functional testing of the system.